Chapter 19
Optimal Design of Large-Scale Frame Structures

19.1 Introduction

Discrete or continuous size optimization of large-scale, high-rise, or complex structures leads to problems with large number of design variables and large search spaces and requires the control of a great number of design constraints. Separate design decisions for each variable would be allowed. Thus, the optimizer invoked to process such a sizing problem is given the possibility to really optimize the objective function by detecting the optimum solution within a vast amount of possible design options. The huge number of available design options typically confuses an optimizer and radically decreases the potential of effective search for a high-quality solution. This chapter is based on the recent development on design of large-scale frame structures (Kaveh and Bolandgerami [1]).

Various optimization approaches have been investigated and successfully applied to optimum design of large-scale structures in the recent years. Classical optimization algorithms (Schulz and Book [2]; Dreyer et al. [3]; Wang and Arora [4]) for large-scale problems need many powerful computational systems. Furthermore, many of such algorithms are known as local optimizer, and their final results cannot be considered as the global optimum. Contrary to mathematical programming algorithms, there are metaheuristic algorithms which are often stochastic algorithms and can efficiently explore the search space of the large-scale problems.

Yang et al. [5] proposed a new cooperative coevolution framework that is capable of optimizing large-scale non-separable problems. A random grouping scheme and adaptive weighting are introduced in problem decomposition and coevolution. Instead of conventional evolutionary algorithms, a novel differential evolutionary algorithm was adopted. Hsieh et al. [6] presented a variation on the traditional PSO algorithm, so-called the efficient population utilization strategy for particle swarm optimization (EPUS-PSO) for solving large-scale global optimization. This is achieved by using variable particles in swarms to enhance the searching ability and drive particles more efficiently. Moreover, sharing principals are

A. Kaveh, *Advances in Metaheuristic Algorithms for Optimal Design of Structures*,
DOI 10.1007/978-3-319-46173-1_19

constructed to stop particles from falling into the local minimum and make the global optimal solution easier to find by particles. Fister et al. [7] used memetic computation (MC) which is emerged recently as a new paradigm of efficient algorithms for solving the hardest optimization problems. Artificial bee colony algorithm and memetic computation are used under the same roof. As a result, a memetic artificial bee colony algorithm (MABC) algorithm has been developed to solve large-scale global optimization problems. Self-organizing migrating algorithm with quadratic interpolation (SOMAQI) has been extended by Singha and Agrawalb [8] to solve large-scale global optimization problems for dimensions ranging from 100 to 3000 with a constant population size of 10 only. This produces high-quality optimal solution with very low computational cost and converges very fast to optimal solution.

In particular, some researchers have performed optimization on large-scale structures. Kaveh and Talatahari [9] introduced a modified version of the charged system search for large structure optimization which was based on the combination of charged system search algorithm and particle swarm optimization. Lagaros [10] presented a computing platform for real-world and large-scale structures. Talatahari and Kaveh [11] introduced an improved bat algorithm for optimizing large-scale structures. Aydogdu et al. [12] improved the performance of artificial bee colony algorithm by adding Lévy flight distribution in the search of scout bees and successfully applied to large steel space frames. Except improving the algorithm, other methods have been proposed. For example, Papadrakakis et al. [13] used neural network in order to replace the structural analysis phase and to compute the necessary data for the evolution strategies optimization procedure. The use of neural network was motivated by the time-consuming repeated analyses required by ES during the optimization process.

In order to overcome the dilemma of using large design variables, in addition to modifying or introducing new optimization algorithms, some methods have been proposed in literature. Sobieszczanski-Sobieski et al. [14] introduced a multilevel optimization and generalized multilevel optimization (Sobieszczanski-Sobieski et al. [15]) which break large optimization problems into several smaller subproblems, and a coordination problem is formulated to preserve the couplings among these subproblems. A very important benefit of such an approach, in addition to making the entire problem more tractable, is preservation of the customary organization of the design office in which many engineers work concurrently on different parts of the problem. Charmpis et al. [16] employed the concept of cascading, allowing a single optimization problem to be tackled in a number of successive autonomous optimization stages. Under this context, several coarse versions of the same full-size database are formed, in order to utilize a different database in each cascade stage executed with an evolutionary optimization algorithm. The early optimization stages of the resulting multi-database cascade procedure make use of the coarsest database versions available and serve the purpose of the basic design space exploration. The last stages exploit finer databases (including the original full-size database) and aim in fine-tuning to achieve optimal solution.

Optimum design of large-scale dome trusses using cascade optimization has been carried out by Kaveh and Ilchi Ghazaan [17].

Cascade sizing optimization utilizing a series of design variable configurations (DVCs) is used in this study. Several design variable configurations are constructed, in order to utilize a different configuration at each cascade optimization stage. Each new cascade stage is coupled with the previous one by initializing the new stage using the finally attained optimum design of the previous one. The early optimization stages of the cascade procedure make use of the coarsest configurations with small numbers of design variables and serve the purpose of basic design space exploration. The last stages exploit finer configurations with larger numbers of design variables and aim in fine-tuning the achieved optimal solution.

Utilized optimizer in all stages of the cascade process is enhanced colliding bodies optimization (ECBO) which is introduced by Kaveh and Ilchi Ghazaan [18]. However, any other metaheuristic algorithm could be used. Colliding bodies optimization (CBO) which is introduced by Kaveh and Mahdavi [19] is a new multi-agent algorithm inspired by a collision between two objects in one dimension. Each agent is modeled as a body with a specified mass and velocity. A collision occurs between pairs of objects, and the new positions of the colliding bodies are updated based on the collision laws. Enhanced colliding bodies optimization (ECBO) uses memory to save some best solutions and has a mechanism to escape from local optima.

The present chapter is organized as follows. Code-based design optimization of steel frames is presented in Sect. 19.2. Section 19.3 introduces cascade sizing optimization utilizing a series of design variable configurations. CBO algorithm and its enhanced version are introduced in Sect. 19.4. In Sect. 19.5, optimal designs of three large-scale space frames with the proposed approach are investigated. Finally, some conclusions are derived in Sect. 19.6.

19.2 Code-Based Design Optimization of Steel Frames

For a steel frame structure consisting of N_m members that are collected in N_d design groups (variables), the optimum design problem according to ASD-AISC (American Institute of Steel Construction [20]) code yields the following discrete programming problem, if the design groups are selected from steel sections in a given profile list.

Find a vector of integer values $\boldsymbol{I}$ representing the sequence numbers of steel sections assigned to N_d member groups as:

$$\boldsymbol{I}^T = [I_1, I_2, \ldots, I_{N_d}] \tag{19.1}$$

to minimize the weight (W) of the frame:

$$W = \sum_{i=1}^{N_d} \rho_i A_i \sum_{j=1}^{N_t} L_j \tag{19.2}$$

where A_i and ρ_i are the area and unit weight of the steel section adopted for member group i, respectively, N_t is the total number of members in group i, and L_j is the length of the member j which belongs to the group i.

The members subjected to a combination of axial compression and flexural stress must be sized to meet the following stress constraints:

$$\text{if } \frac{f_a}{F_a} > 0.15; \quad \left[\frac{f_a}{F_a} + \frac{C_{mx} f_{bx}}{\left(1 - \frac{f_a}{F'_{ex}}\right) F_{bx}} + \frac{C_{my} f_{by}}{\left(1 - \frac{f_a}{F'_{ey}}\right) F_{by}}\right] - 1 \leq 0 \tag{19.3}$$

$$\left[\frac{f_a}{0.60\, F_y} + \frac{f_{bx}}{F_{bx}} + \frac{f_{by}}{F_{by}}\right] - 1 \leq 0 \tag{19.4}$$

$$\text{if } \frac{f_a}{F_a} < 0.15; \quad \left[\frac{f_a}{F_a} + \frac{f_{bx}}{F_{bx}} + \frac{f_{by}}{F_{by}}\right] - 1 \leq 0 \tag{19.5}$$

If the flexural member is under tension, then the following formula is used instead:

$$\left[\frac{f_a}{0.60\, F_y} + \frac{f_{bx}}{F_{bx}} + \frac{f_{by}}{F_{by}}\right] - 1 \leq 0 \tag{19.6}$$

In Eqs. (19.3) and (19.6), F_y is the material yield stress, and $f_a = (P/A)$ represents the computed axial stress, where A is the cross-sectional area of the member. The computed flexural stresses due to bending of the member about its major (x) and minor (y) principal axes are denoted by f_{bx} and f_{by}, respectively. F'_{ex} and F'_{ey} denote the Euler stresses about principal axes of the member that are divided by a factor of safety of 23/12. F_a stands for the allowable axial stress under axial compression force alone and is calculated depending on elastic or inelastic bucking failure mode of the member using Formulas 1.5-1 and 1.5-2 of ASD-AISC. The allowable bending compressive stresses about major and minor axes are designated by F_{bx} and F_{by}, which are computed using Formulas 1.5-6a or 1.5-6b and 1.5-7 provided in ASD-AISC. C_{mx} and C_{my} are the reduction factors, introduced to counterbalance overestimation of the effect of secondary moments by the amplification factor $(1 - f_a/F'_e)$. For braced frame members without transverse loading between their ends, these are calculated from $C_m = 0.6 - 0.4\,(M_1/M_2)$, where M_1/M_2 is the ratio of smaller end moment to the larger end moment. For braced frame members having transverse loading between their ends, these are determined from the formula $C_m = 1 + \psi\left(f_a/F'_e\right)$ based on a rational approximate analysis outlined in ASD-AISC Commentary-H1, where ψ is a parameter that considers maximum deflection and maximum moment in the member.

For computation of allowable compression and Euler stresses, the effective length factors K are required. For beam and bracing members, K is taken equal to unity. For column members, alignment charts furnished in ASD-AISC can be utilized. In this study, however, the effective length factors of columns in a braced frame are calculated from the following approximate formula developed by Dumonteil [21], which are accurate within about $-1.0\,\%$ and $+2.0\,\%$ of the exact results (Hellesland [22]):

$$K = \frac{3G_AG_B + 1.4(G_A + G_B) + 0.64}{3G_AG_B + 2.0(G_A + G_B) + 1.28} \tag{19.7}$$

where G_A and G_B refer to the stiffness ratio or relative stiffness of a column at its two ends.

It is also required that computed shear stresses (f_v) in members should be smaller than the allowable shear stresses (F_v), as formulated in Eq. (19.8):

$$f_v \leq F_v = 0.40C_vF_y \tag{19.8}$$

In the above equation, C_v is referred to as web shear coefficient. It is taken equal to $C_v = 1.0$ for the rolled W-shaped members with $h/t_w \leq 2.24E/F_y$, where h is the clear distance between flanges, E is the elasticity modulus, and t_w is the thickness of web. For all other symmetric shapes, C_v is calculated from Formulas G2-3, G2-4, and G2-5 in ANSI/AISC 360-05 (Specification [23]).

Apart from stress constraints, slenderness limitations are also imposed on all members such that the maximum slenderness ratio ($\lambda = KL/r$) is limited to 300 for members under tension and to 200 for members under compression loads. The displacement constraints are imposed such that the maximum lateral displacements are restricted to be less than $H/400$ and the upper limit of story drift is set to be $h/400$, where H is the total height of the frame building and h is the height of a story.

Finally, we consider geometric constraints between beams and columns framing into each other at a common joint for practicality of an optimum solution generated. For the two beams $B1$ and $B2$ and the column shown in Fig. 19.1, one can write the following geometric constraints:

$$\frac{b_{fb}}{b_{fc}} - 1.0 \leq 0 \tag{19.9}$$

$$\frac{b'_{fb}}{(d_c - 2t_f)} - 1.0 \leq 0 \tag{19.10}$$

where b_{fb}, b'_{fb}, and b_{fc} are the flange width of the beam $B1$, the beam $B2$, and the column, respectively; d_c is the depth of the column; and t_f is the flange width of the column. Equation (19.9) simply ensures that the flange width of the beam $B1$ remains smaller than that of the column. On the other hand, Eq. (19.10) guarantees

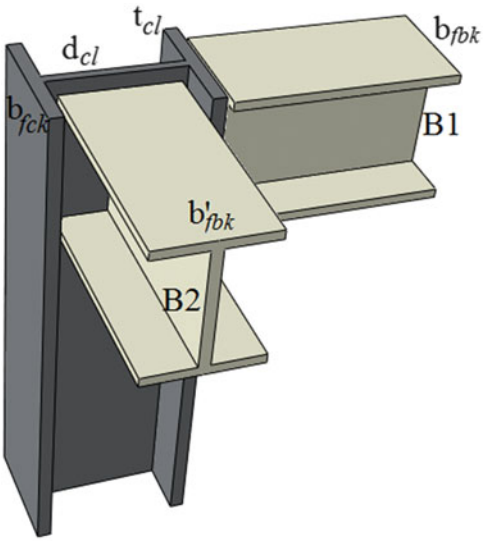

Fig. 19.1 Schematic of a beam–column geometric constraints [1]

that flange width of the beam *B2* remains smaller than clear distance between the flanges of the column ($d_c - 2t_f$).

19.3 Cascade Sizing Optimization Utilizing a Series of Design Variable Configurations

Cascade sizing optimization approach utilized in this work is presented in this section. First, the concept of cascade optimization is introduced, and then multi-design variable configuration (DVC) cascade optimization is presented.

19.3.1 Cascade Optimization Strategy

There is no unique optimization algorithm capable of effectively solving all optimization problems. Cascade optimization strategy has been introduced as a multi-stage procedure, which employs various optimizers in a successive manner to solve an optimization problem (Patnaik et al. [24]). Each autonomous optimization stage of the cascade procedure starts from an initial design, which is either a "cold start" or a "hot start." The early stage starts from cold start which is a user-specified or randomly selected design. After running the early-stage optimizer, the optimal solution reached is used as the starting solution for the second cascade stage. This new starting solution is called a hot start, because during the execution of the initial optimizer, the achieved optimal solution has moved toward the region of the global

optimum. Then, each optimization stage of the cascade procedure starts from the optimum solution achieved at the previous stage.

The actual aim of cascading is to take advantage of the combined strength and the differentiated computations of a number of optimizers executed in a successive manner. This advantage has been used for structural sizing optimization (Charmpis et al. [16], Lagaros [10], Kaveh and Ilchi Ghazaan [17]).

19.3.2 Multi-DVC Cascade Optimization

Multi-DVC cascade optimization method employs a series of configurations for the design variable configurations (DVCs) of the problem at hand and at each stage of cascade uses from different DVCs. DVCs are defined in a manner that DVCs used in early stages have less design variables than DVCs utilized in final stages. The early stage of the cascade procedure executed with the coarsest DVCs aims at a basic non-detailed search of the entire design space. This search is facilitated by the manageable DVCs handled, which avoid confusing the employed optimizer with huge design spaces although it does not consider a lot of design options. With this method, global search is performed in early stages and more detailed and local search is performed in final stages. The final stage of cascade optimization in this method uses the finest DVC. Figure 19.2 shows the flowchart of the multi-DVC cascade optimization procedure.

DVCs can be generated based on engineering experience. Here, variables of one kind (exterior beams, interior beams, corner columns, etc.) for some stories are integrated in coarser DVC, while in finer DVC structural members are grouped separately for each story.

For each stage of the cascade optimization method, one can choose different optimization algorithm. Choosing an optimization algorithm which is capable in global search for early stages and local search algorithms for final stages may result in a better cascade method performance. However, in this chapter enhanced colliding bodies optimization, presented in the subsequent section, is used as the optimization algorithm in all the stages of the cascade optimization.

In order to explain the utilized method (without loss of generality), consider three stages of the cascade procedure. In this method, C_0 is the number of DVCs that is defined by the problem, so two other coarser DVCs should be defined (C_1 and C_2). In the first stage of the cascade procedure, the first optimizer works with C_2 which is the coarsest DVC and finally attains $d_1(C_2)$ design. In the first stage, optimizer deals with relatively small number of variables and thus in a reasonable number of iterations achieves the $d_1(C_2)$ design. $d_1(C_2)$ is a vector with $n_d(C_2)$ entries, and before starting the second stage of cascade procedure, $d_1(C_2)$ must be converted to the vector $d_1(C_1)$ with $n_d(C_1)$ entries. For this conversion, design information of each structural member should be extracted. Notation n_d refers to the number of design variables in each DVC. After conversion, the second optimizer in the second stage of the cascade procedure starts from $d_1(C_1)$ and achieves

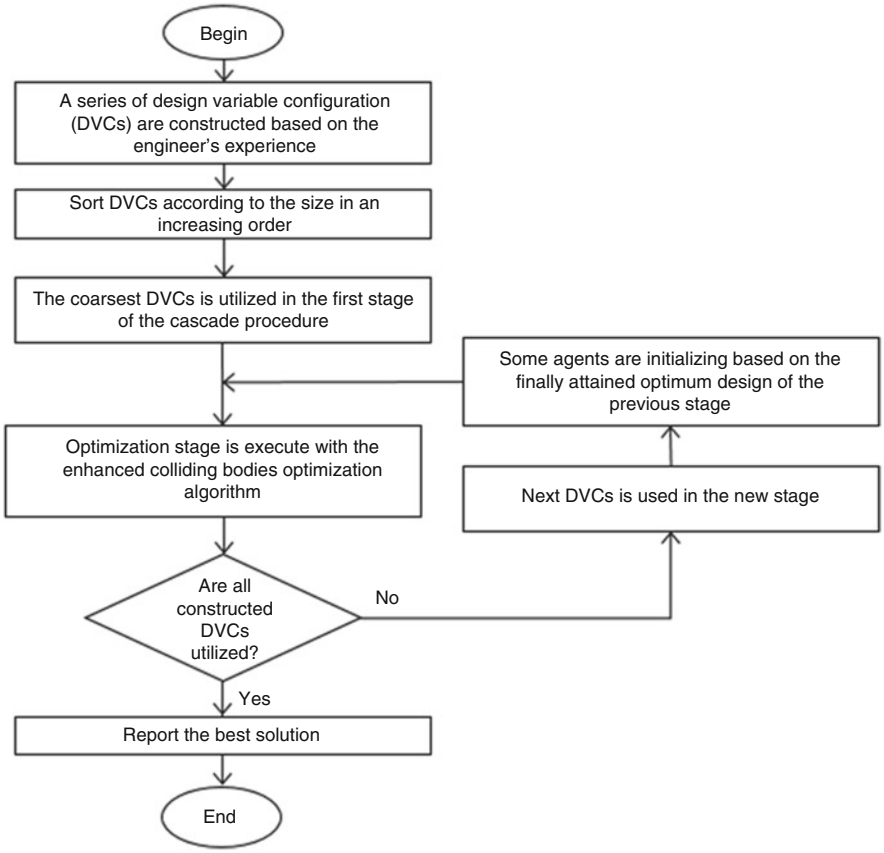

Fig. 19.2 Flowchart of the multi-DVC cascade optimization procedure [1]

the $d_2(C_1)$. Due to the second optimizer efforts in the second stage of the cascade procedure, d_2 will have better fitness value than d_1. Finally, in the third stage of the cascade method, the third optimizer starts from $d_2(C_0)$ and achieves the $d_3(C_0)$. Here, the $d_2(C_0)$ is the converted vector of the $d_2(C_1)$, and d_3 is the best achieved design in all stages of the cascade procedure.

For basic and non-detailed search of all region of design space, the first stages of cascade procedure executed with the coarsest DVCs. Due to relatively small number of design variables in the coarsest DVCs, optimizer will not be confused and search can be facilitated by the manageable DVCs handled. Accordingly, the appropriate regions of design space are identified by detecting optimum solutions among the relatively limited design options provided. With increasing numbers of design variables in the next stages of cascade procedure, more detailed search will be available, and the optimizer is given the opportunity to improve the quality of the optimal solution reached. Optimal design vector over a number of cascade stages is upgraded gradually by the transfer of optimization results between successive

stages. Although in the last stages of cascade procedure optimizer deals with large number of design variables, the appropriate initialization of each cascade stage prevents the optimizer from being trapped in a process of purposeless and ineffective searching. Hence, the first optimization stages of the cascade procedure serve the purpose of basic design space exploration, while the last stages aim in fine-tuning the achieved optimal solution.

19.4 Colliding Bodies Optimization and Its Enhanced Version

19.4.1 A Brief Explanation of the CBO Algorithm

The colliding bodies optimization (CBO) is a metaheuristic algorithm introduced by Kaveh and Mahdavi [19] and contains a number of colliding bodies (CB) where each one collides with other objects to explore the search space. In CBO, each solution candidate Xi containing a number of variables (i.e., Xi = {Xi,j}) is considered as a colliding body (CB). In discrete problems, CBs are allowed to select discrete values from a list. Actually, real numbers are rounded to the nearest integer.

Each CB is a solution candidate so its objective function (here, weight of structure multiplied by the penalty function) value can be calculated. In this way, constraints are applied using a penalty function. CBs according to their objective function values take specified mass defined as:

$$m_k = \frac{\frac{1}{fit(k)}}{\frac{1}{\sum_{i=1}^{n}\frac{1}{fit(i)}}}, \quad k=1,\ 2,\ \ldots,n \tag{19.11}$$

where *fit (i)* represents the objective function value of the *i*th CB and *n* is the number of colliding bodies. Thus, in each iteration, all the CBs must be evaluated. Here, finite element analysis constraints check must be performed.

After sorting colliding bodies according to their objective function values in an increasing order, two equal groups are created: (i) stationary group and (ii) moving group (Fig. 19.3). Moving objects collide to stationary objects to improve their positions and push stationary objects toward better positions. The velocities of the stationary and moving bodies before collision (v_i) are calculated by:

$$v_i = 0, \quad i = 1,\ 2,\ \ldots,\frac{n}{2} \tag{19.12}$$

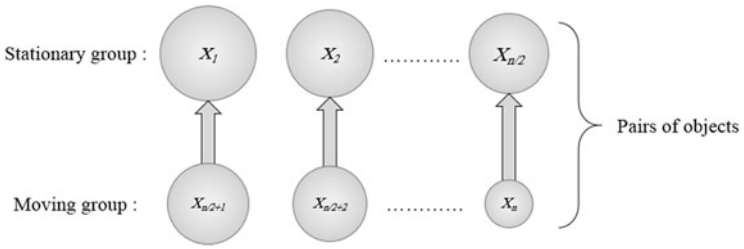

Fig. 19.3 Pairs of CBs for collision

$$v_i = x_{i-\frac{n}{2}} - x_i, \quad i = \frac{n}{2} + 1, \frac{n}{2} + 2, \ \ldots, \ n \tag{19.13}$$

where x_i is the position vector of the ith CB.

The velocities of stationary and moving CBs after the collision (v'_i) are evaluated by:

$$v'_i = \frac{\left(m_{i+\frac{n}{2}} + \varepsilon m_{i+\frac{n}{2}}\right) v_{i+\frac{n}{2}}}{m_i + m_{i+\frac{n}{2}}} \quad i = 1, 2, \ \ldots, \frac{n}{2} \tag{19.14}$$

$$v'_i = \frac{\left(m_i - \varepsilon m_{i-\frac{n}{2}}\right) v_i}{m_i + m_{i-\frac{n}{2}}} \quad i = \frac{n}{2} + 1, \frac{n}{2} + 2, \ \ldots n \tag{19.15}$$

$$\varepsilon = 1 - \frac{iter}{iter_{max}} \tag{19.16}$$

where ε is the coefficient of restitution (COR) and $iter$ and $iter_{max}$ are the current iteration number and the total number of iterations for optimization process, respectively.

New positions of each group are stated by the following formulas:

$$x_i^{new} = x_i + rand \circ v'_i, \quad i = 1, \ 2, \ \ldots, \frac{n}{2} \tag{19.17}$$

$$x_i^{new} = x_{i-\frac{n}{2}} + rand \circ v'_i, \quad i = \frac{n}{2} + 1, \frac{n}{2} + 2, \ \ldots, \ n \tag{19.18}$$

where x_i^{new}, x_i, and $v_i^{'}$ are the new position, the previous position, and the velocity after the collision of the ith CB, respectively; *rand* is a random vector uniformly distributed in the range of $(-1, 1)$ and the sign "$\circ$" denotes an element-by-element multiplication.

The flowchart of CBO algorithm is depicted in Fig. 19.4.

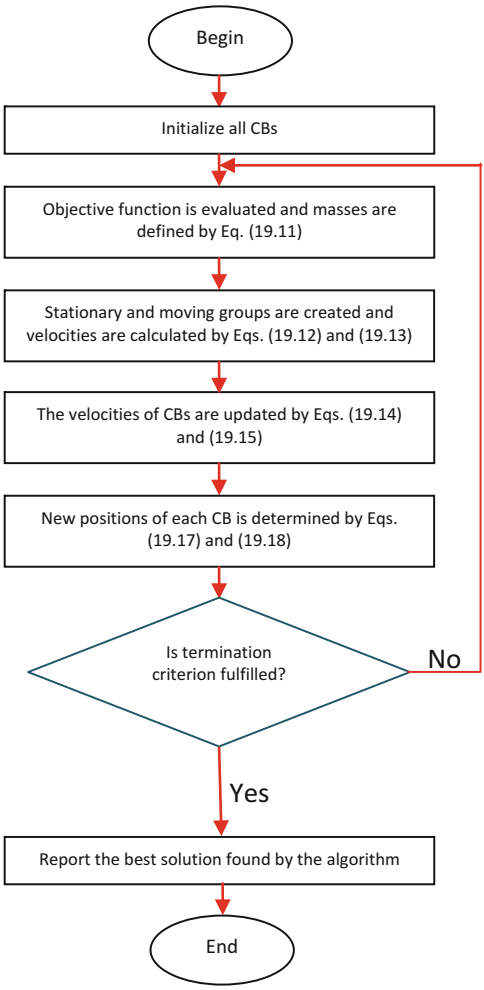

Fig. 19.4 Flowchart of the CBO algorithm

19.4.2 The ECBO Algorithm

The enhanced version of the CBO is introduced by Kaveh and Ilchi Ghazaan [18]. In the enhanced colliding bodies optimization (ECBO), a memory that saves a number of historically best CBs is utilized to improve the performance of the CBO and to reduce the computational cost. Furthermore, ECBO changes some components of the CBs randomly to prevent premature convergence. In order to introduce the ECBO, the following steps are developed and the corresponding flowchart is provided in Fig. 19.5.

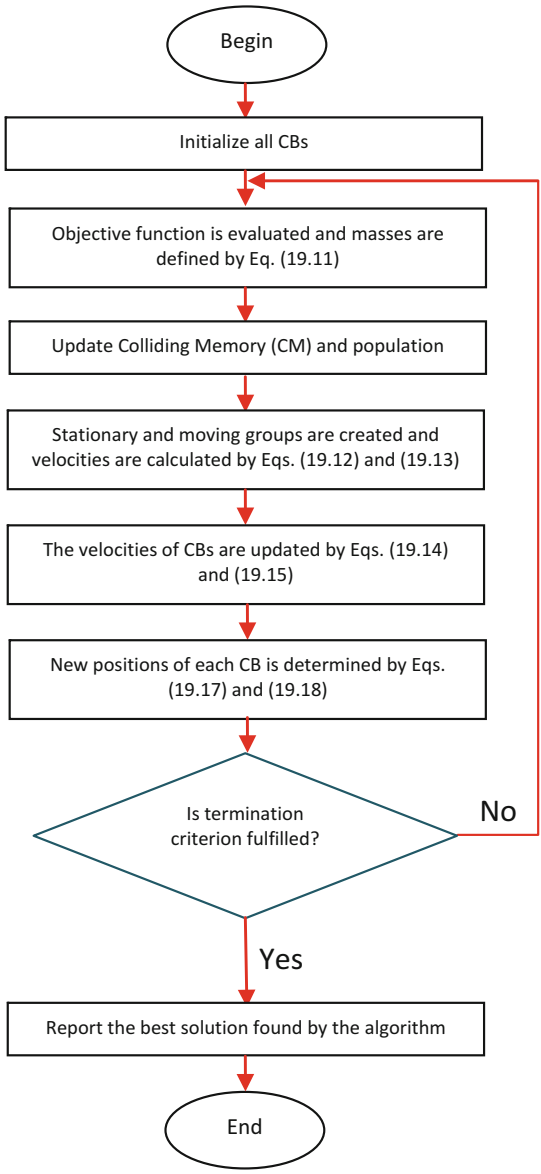

Fig. 19.5 Flowchart of the ECBO algorithm

Level 1: Initialization

Step 1: The initial locations of CBs are created randomly in an m-dimensional search space.

$$x_i^0 = x_{min} + random_\circ\,(x_{max} - x_{min}), \quad i = 1,\ 2,\ \ldots, n \tag{19.19}$$

where $x_i^{\,0}$ is the initial solution vector of the ith CB, x_{min} and x_{max} are the minimum and the maximum allowable variable vectors, and random is a random vector with each component being in the interval [0, 1].

Level 2: Search

Step 1: The value of the mass for each CB is calculated by Eq. (19.11).

Step 2: Colliding memory (CM) is considered to save some historically best CB vectors and their related mass and objective function values. The size of the *CM* is taken as $n/10$ in this study. At each iteration, solution vectors that are saved in the CM are added to the population, and the same number of the current worst CBs is deleted.

Step 3: CBs are sorted according to their objective function values in an increasing order. To select the pairs of CBs for collision, they are divided into two equal groups: (i) stationary group and (ii) moving group (Fig. 19.3).

Step 4: The velocities of stationary and moving bodies before collision are evaluated in Eqs. (19.12) and (19.13), respectively.

Step 5: The velocities of stationary and moving bodies after collision are calculated in Eqs. (19.14) and (19.15), respectively.

Step 6: The new location of each CB is evaluated by Eq. (19.17) or Eq. (19.18).

Step 7: A parameter like **pro** within (0, 1) is introduced and specified whether a component of each CB must be changed or not. For each CB **pro** is compared with rn_i $(i = 1, 2, \ldots, n)$ which is a random number uniformly distributed within (0, 1). If $rn_i < \mathbf{pro}$, one dimension of the ith CB is selected randomly and its value is regenerated by:

$$x_{ij} = x_{j,min} + random\ .\ \left(x_{j,max} - x_{j,min}\right) \tag{19.20}$$

where x_{ij} is the jth variable of the ith CB and $x_{j,min}$ and $x_{j,max}$ are the lower and upper bounds of the jth variable.

Level 3: Termination Condition Check

Step 1: After the predefined maximum evaluation number, the optimization process is terminated.

This algorithm is used in many papers and its efficiency has been proven in structural size optimization. ECBO algorithm being capable of maintaining a proper balance between the diversification and the intensification inclinations is utilized in all stages of cascade process. Local search algorithms are proper for the last stages of the proposed method, but these cannot have suitable global search in the first stages. Moreover, the ECBO algorithm has recently been used for structural optimization.

Although the idea of cascade procedure has been introduced to be used for multiple optimizers, however, in this chapter another kind of cascade procedure is implemented in which, instead of using multiple optimizers, multiple DVCs are

utilized. The potential of using multiple optimizers has already been shown. For this reason single optimizer is used in all stages of the cascade procedure in order to examine the efficiency of proposed method independent of the utilized optimizers.

19.5 Numerical Examples

Three large-scale steel space frames are studied to investigate the efficiency of the cascade-enhanced colliding bodies optimization in weight optimum design. These examples consist of a 1860-member steel space frame with 72 member groups (design variables), a 3590-member steel space frame with 124 member groups, and finally a 3328-member steel space frame with 186 member groups.

The structural members are sized using wide-flange W-sections, such that columns are selected from the complete set of 297 W-sections, beams are selected from a set of 171 economical W-sections chosen based on area and inertia properties, and finally bracings are selected from a set of 147 economical W-sections chosen based on area and radii of gyration properties. The material properties of the steel are assumed as follows: modulus of elasticity $E = 29{,}000$ ksi (203893.6 MPa) and yield stress $Fy = 36$ ksi (253.1 MPa). Design constraints and objective function are considered as defined in Sect. 19.2.

The objective function utilized is as follows:

$$fit\,(x) = W(x)\ \times (1 + \upsilon) \tag{19.21}$$

$$\upsilon = \sum\nolimits_{i=1}^{nc} max[0, g_i(x)] \tag{19.22}$$

where W is the weight of the structure obtained using Eq. (19.2) and g contains all the constraints mentioned in Sect. 19.2. In colliding bodies optimization algorithm, the value of the objective function for each candidate is obtained using the above equations, and these values are incorporated in calculating the mass of the colliding bodies (Eq. (19.11)).

For all examples, **pro** parameter in ECBO is set to 0.3 and a population of 40 CBs is implemented. Colliding memory (CM) size for non-cascade ECBO and cascade ECBO is set to 2 and 3, respectively, and three best attained designs are moved to the next stage in the cascade method. All examples started with a random population. Due to randomness property of the algorithms, five cascade and five non-cascade runs are performed for each example, and the best results, means, and standard deviations are provided.

The algorithms are coded in MATLAB (The MathWorks [25]), and the structures are analyzed using OpenSees (Mazzoni et al. [26]). These two softwares are linked together and static linear finite element analysis is performed in OpenSees (Mazzoni et al. [26]). Then, structural response is received by MATLAB (The MathWorks [25]) to check the constraints and evaluate the objective function values.

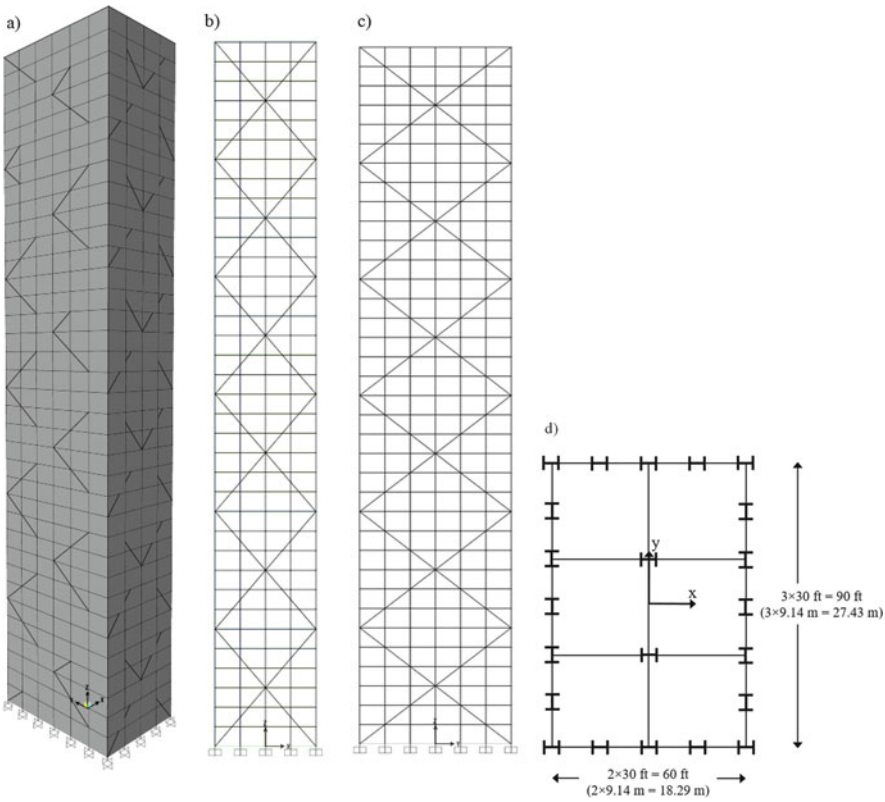

Fig. 19.6 Schematic of a 1860-member braced space steel frame [1]. (**a**) Three-dimensional view, (**b**) front view, (**c**) side view, and (**d**) plan view

19.5.1 A 1860-Member Steel Space Frame

The first design example considered in this section is a 36-story braced space steel frame consisting of 814 joints and 1860 members. This structure has also been investigated by Saka and Hasançebi [27]. The side, plan, and three-dimensional views of the frame are shown in Fig. 19.6. An economical and effective stiffening of the frame against lateral forces is achieved through exterior diagonal bracing members located on the perimeter of the building, which also participate in transmitting the gravity forces.

The 1860 frame members are collected in 72 different member groups, considering the symmetry of the structure and practical fabrication requirements. That is, the columns in each story are collected in three member groups as corner columns, inner columns, and outer columns, whereas beams are divided into two groups as inner beams and outer beams. The corner columns are grouped together as having the same section over three adjacent stories, as inner columns, outer columns, inner beams, and outer beams. Bracing members on each facade are designed as three-

Table 19.1 Number of design variables and their allocation to structural parts for each DVC of the 1860-member braced steel space frame

DVC	Member type	Number of member groups	Total	Remarks
C_0	Columns	$3 \times 12 = 36$	72	Corner columns, inner columns, and outer columns grouped every three stories
	Beams	$2 \times 12 = 24$		Outer beams and inner beams grouped every three stories
	Bracings	$2 \times 6 = 12$		Bracings in x direction and y direction grouped every six stories
C_1	Columns	$3 \times 6 = 18$	34	Corner columns, inner columns and outer columns grouped every six stories
	Beams	$2 \times 6 = 12$		Outer beams and inner beams grouped every six stories
	Bracings	$2 \times 2 = 4$		Bracings in x direction and y direction grouped every 18 stories
C_2	Columns	$3 \times 2 = 6$	10	Corner columns, inner columns, and outer columns grouped every 18 stories
	Beams	$2 \times 1 = 2$		Outer beams and inner beams grouped in all stories
	Bracings	$2 \times 1 = 2$		Bracings in x direction and y direction grouped in all stories

story deep members, and two bracing groups are specified in every six stories. Table 19.1 shows the number of design variables and their allocation in structural parts for each of the three DVCs defined for cascade method.

The 1860-member braced space steel frame is subjected to two loading conditions of combined gravity and wind forces. These forces are computed as per ASCE 7-05 based on the following design values: a design dead load of 2.88 kN/m^2 (60.13 lb/ft^2), a design live load of 2.39 kN/m^2 (50 lb/ft^2), a ground snow load of 1.20 kN/m^2 (25 lb/ft^2), and a basic wind speed of 55.21 m/s (123.5 mph). Lateral (wind) loads acting at each floor level on windward and leeward faces of the frame are tabulated in Table 19.2, and the gravity loading on the beams of roof and floors is given in Table 19.3. In the first loading condition, gravity loads are applied together with wind loads acting along x-axis (1.0 GL + 1.0WL-x), whereas in the second one, they are applied with wind loads acting along y-axis (1.0 GL + 1.0WL-y).

The 1860-member braced space steel frame is designed separately by using both ECBO and cascade ECBO search method. The maximum number of analyses was 30,000. The design history of both runs is shown in Fig. 19.7. The minimum weight for the frame is determined as 4637.45 klb by the cascade ECBO method, while non-cascade ECBO arrived at 6406.53 klb which is 38.1 % heavier. The mean and standard deviation of the independent runs for cascade optimization procedure are 4647.10 klb and 18.37 klb, respectively, whereas the values of these parameters for non-cascade procedure are 6420.53 klb and 25.54 klb, respectively. Figure 19.8 shows the ratio of story drift over the maximum allowable drift of the story for final

Table 19.2 Wind loading on a 1860-member braced space steel frame

Floor	Windward kN/m (lb/ft)	Leeward kN/m (lb/ft)
1	2.05 (140.64)	3.57 (244.70)
2	2.50 (171.44)	3.57 (244.70)
3	2.81 (192.49)	3.57 (244.70)
4	3.05 (208.98)	3.57 (244.70)
5	3.25 (222.74)	3.57 (244.70)
6	3.42 (234.65)	3.57 (244.70)
7	3.58 (245.22)	3.57 (244.70)
8	3.72 (254.75)	3.57 (244.70)
9	3.85 (263.47)	3.57 (244.70)
10	3.96 (271.52)	3.57 (244.70)
11	4.07 (279.02)	3.57 (244.70)
12	4.18 (286.04)	3.57 (244.70)
13	4.27 (292.66)	3.57 (244.70)
14	4.36 (298.92)	3.57 (244.70)
15	4.45 (304.87)	3.57 (244.70)
16	4.53 (310.55)	3.57 (244.70)
17	4.61 (315.97)	3.57 (244.70)
18	4.69 (321.18)	3.57 (244.70)
19	4.76 (326.18)	3.57 (244.70)
20	4.83 (330.99)	3.57 (244.70)
21	4.90 (335.64)	3.57 (244.70)
22	4.97 (340.13)	3.57 (244.70)
23	5.03 (344.48)	3.57 (244.70)
24	5.09 (348.69)	3.57 (244.70)
25	5.15 (352.78)	3.57 (244.70)
26	5.21 (356.76)	3.57 (244.70)
27	5.27 (360.62)	3.57 (244.70)
28	5.32 (364.39)	3.57 (244.70)
29	5.37 (368.06)	3.57 (244.70)
30	5.43 (371.65)	3.57 (244.70)
31	5.48 (375.14)	3.57 (244.70)
32	5.53 (378.56)	3.57 (244.70)
33	5.58 (381.90)	3.57 (244.70)
34	5.62 (385.18)	3.57 (244.70)
35	5.67 (388.38)	3.57 (244.70)
36	2.86 (195.76)	1.79 (122.35)

Table 19.3 Gravity loading on the beams of 1860-member braced steel space frame

	Uniformly distributed load, kN/m (lb/ft)		
Beam type	Dead load	Live load	Snow load
Roof beams	22.44 (1536.66)	N/A	5.88 (402.50)
Floor beams	22.44 (1536.66)	18.66 (1277.78)	N/A

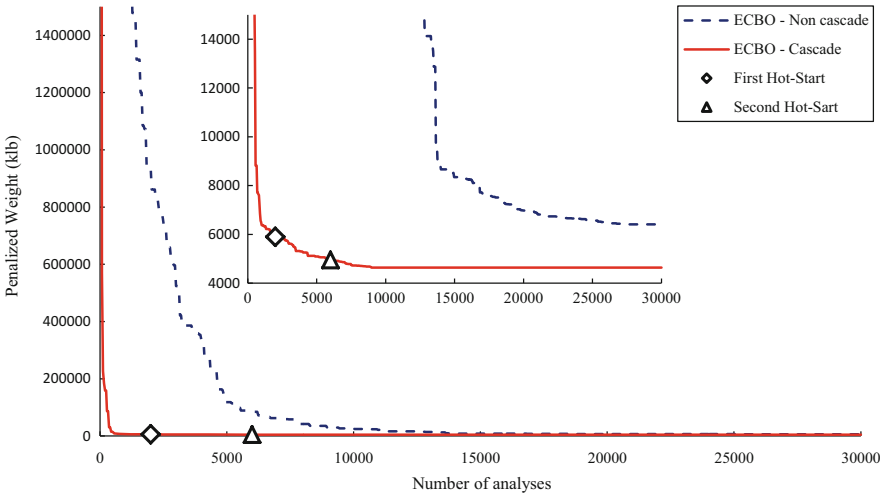

Fig. 19.7 Convergence curves for the 1860-member steel space frame

design of two mentioned methods. In Fig. 19.9 maximum values of stress ratio for members of each design group for ECBO and cascade ECBO are also compared.

Multi-DVC cascade procedure provides some other options for the designer. The designer can choose more uniform structure by spending high cost for materials (that may cause to less final cost). In the first example, attained optimal design with C_1 DVC which contains 34 types of frame sections is only 6.66 % heavier than finally attained design which contains 72 types of frame section.

19.5.2 A 3590-Member Steel Space Frame

The second design example is a braced space steel frame consisting of 1540 joints and 3590 members that are to be built in three adjacent blocks with 30, 18, and 12 stories. The three-dimensional and plan views of the frame at different story levels are shown in Fig. 19.10. An economical and effective stiffening of the frame against lateral forces is achieved through exterior diagonal bracing members located on the perimeter of the building as well as on the adjacent sides of the blocks. The diagonal members are also known to participate in transmitting gravity forces. The 3590 frame members are collected in 124 different member groups altogether. Table 19.4 shows the member groups for this example and two other built DVCs.

The combined stress, stability, and geometric constraints are imposed according to the defined provisions in Sect. 19.2. Similar to the previous example, the 1860-member braced space steel frame is subjected to two loading conditions of combined wind and gravity forces which are tabulated in Tables 19.5 and 19.6,

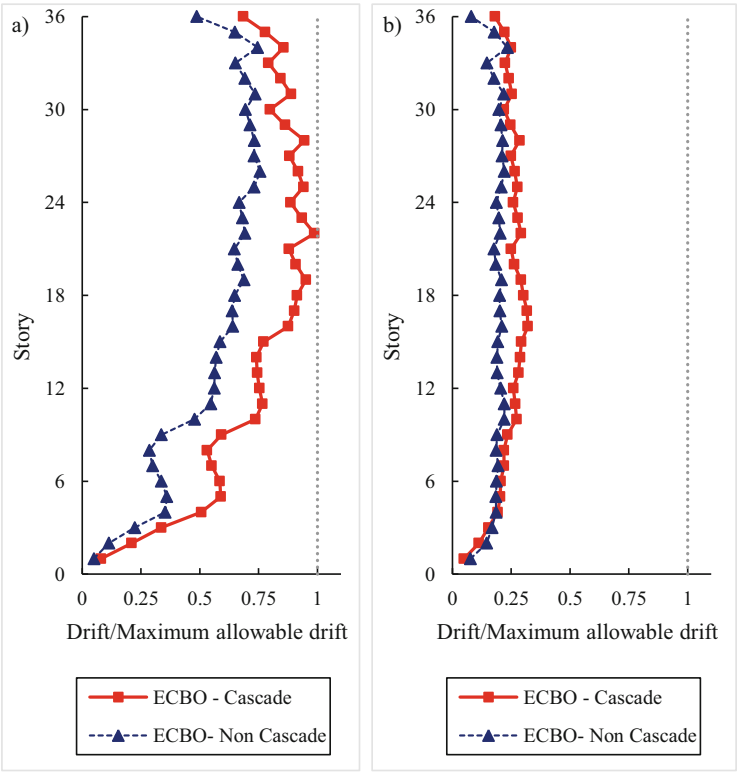

Fig. 19.8 Drift divided by the maximum allowable drift ratio in final design of the 1860-member steel space frame. (**a**) X direction, (**b**) y direction

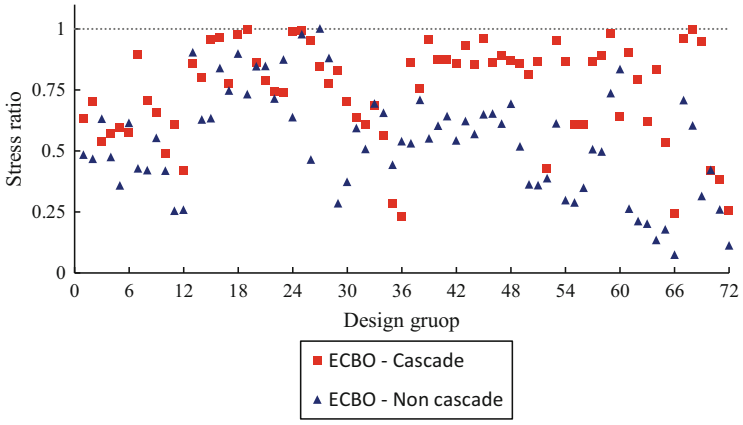

Fig. 19.9 Maximum stress ratio of members in each design group in final design of the 1860-member steel space frame

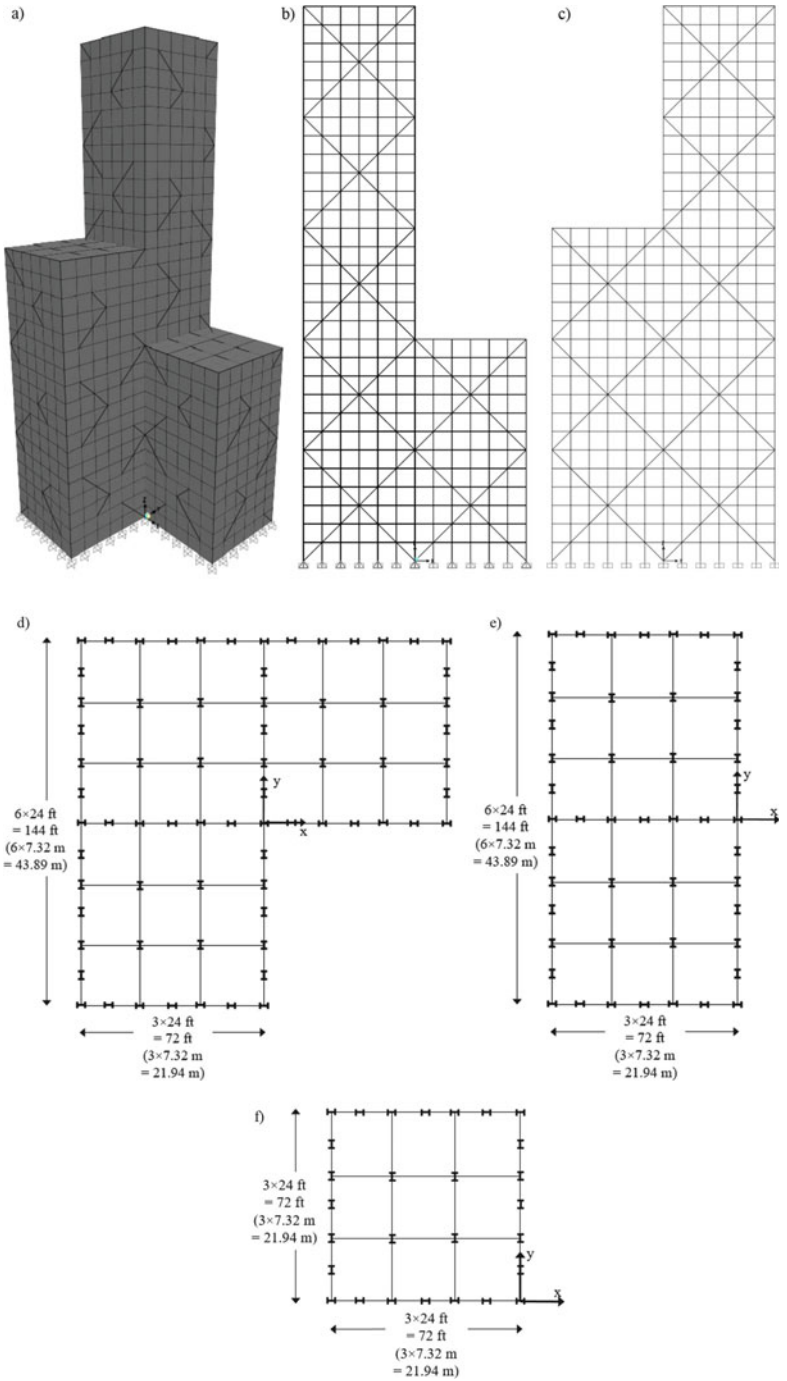

Fig. 19.10 Schematic of a 3590-member braced space steel frame [1]. (**a**) Three-dimensional view, (**b**) front view, (**c**) side view, (**d**) stories 1–12 (Section 1), (**e**) stories 13–18 (Section 2), and (**f**) stories 19–30 (Section 3)

Table 19.4 Number of design variables and their allocation to structural parts for each DVC of the 3590-member braced steel space frame

DVC	Member type	Number of member groups	Total	Remarks
C_0	Columns	$(3 \times 15) + 9 = 54$	124	Corner columns, inner columns, and outer columns grouped every two stories. Inner columns in braced frames are collected in separate groups
	Beams	$2 \times 30 = 60$		Outer beams and inner beams are grouped every story
	Bracings	$1 \times 10 = 10$		Bracings are grouped every three stories
C_1	Columns	$(3 \times 7) + 4 = 25$	60	Corner columns, inner columns, and outer columns in all stories and inner columns in braced fames in Sections 1 and 2 are grouped every four stories. Six above stories are collected in same groups
	Beams	$2 \times 15 = 30$		Outer beams and inner beams grouped every two stories
	Bracings	$1 \times 5 = 5$		Bracings grouped every six stories
C_2	Columns	$(3 \times 2) + 1 = 7$	14	Corner columns, inner columns, and outer columns grouped in 16 below stories and 14 above stories. All inner columns in braced frames are collected in one group
	Beams	$2 \times 3 = 6$		Outer beams and inner beams are grouped in every ten stories
	Bracings	1		All bracings are collected in one group

respectively. In the first loading condition, gravity loads are applied together with wind loads acting along x-axis (1.0 GL + 1.0WL-x), whereas in the second one, these are applied with wind loads acting along y-axis (1.0 GL +1.0WL-y).

An optimum design weight of 6496.41 klb has been reached for the frame with cascade ECBO. Figure 19.11 shows the design history graph for 50,000 analyses obtained for this example. Non-cascade ECBO attained optimum design weight of 9937.94 klb that is 52.98 % heavier than the cascade method design. The mean and standard deviation of the independent runs for cascade optimization procedure are 6505.90 klb and 21.80 klb, respectively, whereas the values of these parameters for non-cascade procedure are 9955.93 klb and 35.67 klb, respectively. Figure 19.12 shows the ratio of story drift over the maximum allowable drift of the story for the final design of two mentioned methods. Maximum values of stress ratios for members of each design group for ECBO and cascade ECBO are also compared in Fig. 19.13.

Table 19.5 Wind loading on the 3590-member braced space steel frame

Floor	Windward kN/m (lb/ft)	Leeward kN/m (lb/ft)
1	1.60 (109.41)	2.47 (169.56)
2	1.83 (125.14)	2.47 (169.56)
3	2.05 (140.51)	2.47 (169.56)
4	2.23 (152.55)	2.47 (169.56)
5	2.37 (162.59)	2.47 (169.56)
6	2.50 (171.28)	2.47 (169.56)
7	2.61 (179.00)	2.47 (169.56)
8	2.71 (185.96)	2.47 (169.56)
9	2.81 (192.32)	2.47 (169.56)
10	2.89 (198.20)	2.47 (169.56)
11	2.97 (203.67)	2.47 (169.56)
12	3.05 (208.80)	2.47 (169.56)
13	3.12 (213.63)	2.47 (169.56)
14	3.18 (218.20)	2.47 (169.56)
15	3.25 (222.54)	2.47 (169.56)
16	3.31 (226.68)	2.47 (169.56)
17	3.37 (230.64)	2.47 (169.56)
18	3.42 (234.44)	2.47 (169.56)
19	3.47 (238.09)	2.47 (169.56)
20	3.53 (241.61)	2.47 (169.56)
21	3.56 (245.00)	2.47 (169.56)
22	3.62 (248.28)	2.47 (169.56)
23	3.67 (251.45)	2.47 (169.56)
24	3.71 (254.53)	2.47 (169.56)
25	3.76 (257.51)	2.47 (169.56)
26	3.80 (260.41)	2.47 (169.56)
27	3.84 (263.24)	2.47 (169.56)
28	3.88 (265.99)	2.47 (169.56)
29	3.92 (268.67)	2.47 (169.56)
30	1.98 (135.64)	84.78)

Table 19.6 Gravity loading on the beams of the 3590-member braced steel space frame

	Uniformly distributed load, kN/m (lb/ft)		
Beam type	Dead load	Live load	Snow load
Roof beams	10.53 (721.56)	N/A	4.38 (300.00)
Floor beams	22.42 (1536.66)	8.76 (600.00)	N/A

19.5.3 A 3328-Member Steel Space Frame

The last design example is a 3328-member irregular moment resisting steel space frame structure with setbacks and cross bracings of Fig. 19.14 which consist of

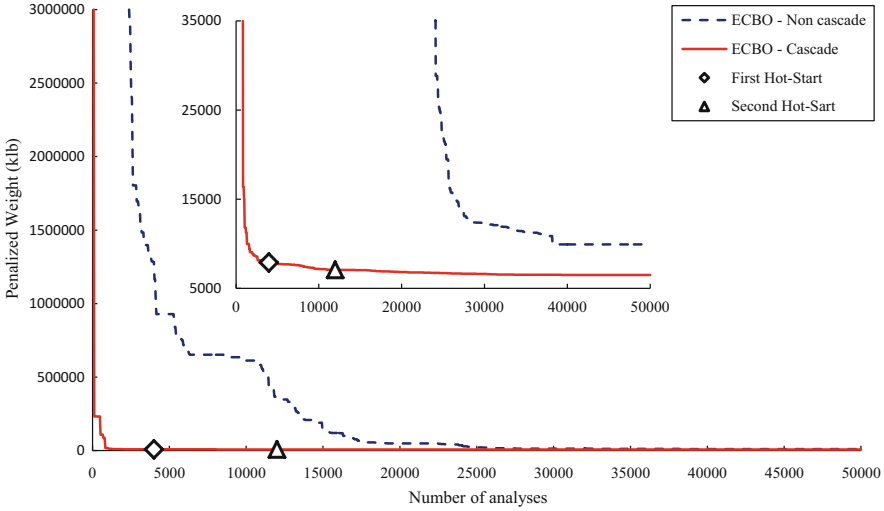

Fig. 19.11 Convergence curves for the 3590-member steel space frame

1384 joints. The space frame is clamped to the ground and is subjected to vertical dead and live loads (Table 19.7) and horizontal wind loads (Table 19.8).

The frame is divided in the vertical direction into three 12-story sections, as shown in Fig. 19.14. Similar structure has been considered by Sarma and Adeli [28]. For this example also two-load combination is defined. In the first loading condition, gravity loads are applied together with wind loads acting along x-axis (1.0 GL + 1.0WL-x), whereas in the second one, they are applied with wind loads acting along y-axis (1.0 GL + 1.0WL-y). Table 19.9 tabulates member groups for the sizing optimization procedure and two other defined DVCs for cascade ECBO method. The following member types of the space frame are distinguished:

- Four types of columns: corner columns, outer columns, inner columns in unbraced frames, and inner columns in braced frames
- Three types of beams for the two lower Sections 1 and 2: outer beams, inner beams in unbraced frames, and inner beams in braced frames
- Two types of beams for the upper Section 3: outer and inner beams
- Two groups of bracings in the longitudinal and transverse directions

Figure 19.15 shows the convergence histories obtained for the proposed cascade ECBO and non-cascade ECBO optimization methods. In this example, 70,000 analyses were executed for cascade and non-cascade ECBO. Non-cascade ECBO attained optimum design weight of 12724.97 klb that is 28.31 % heavier than the cascade method design which attained optimum design weight of 9917.51 klb. The mean and standard deviation of the independent runs for cascade optimization procedure are 9948.72 klb and 43.03 klb, respectively, whereas the values of these parameters for non-cascade procedure are 12772.24 klb and 54.29 klb, respectively. Figure 19.16 shows the ratio of story drift versus the maximum

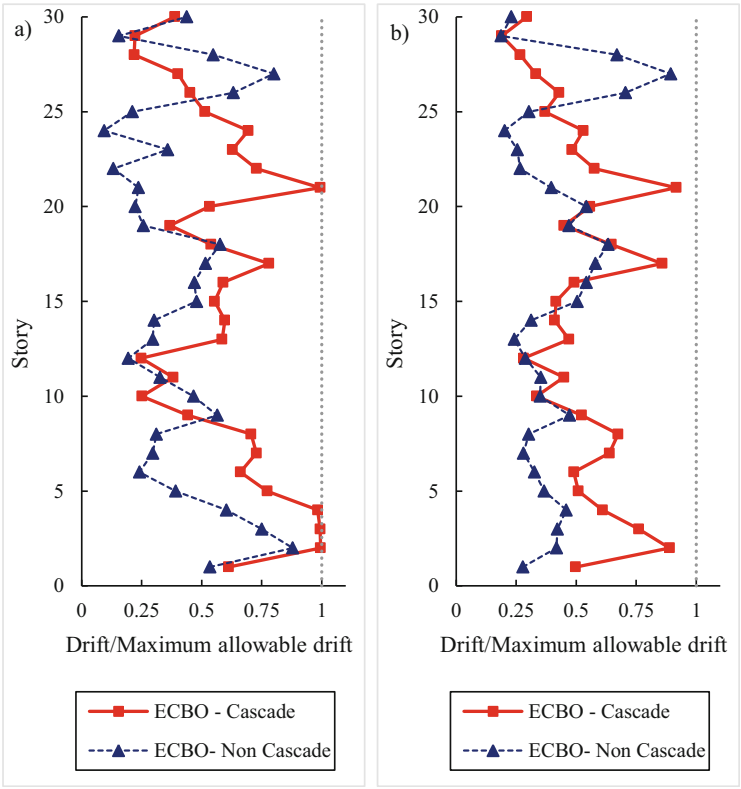

Fig. 19.12 Drift divided by the maximum allowable drift ratio in final design of the 3590-member steel space frame. (**a**) x-direction, (**b**) y-direction

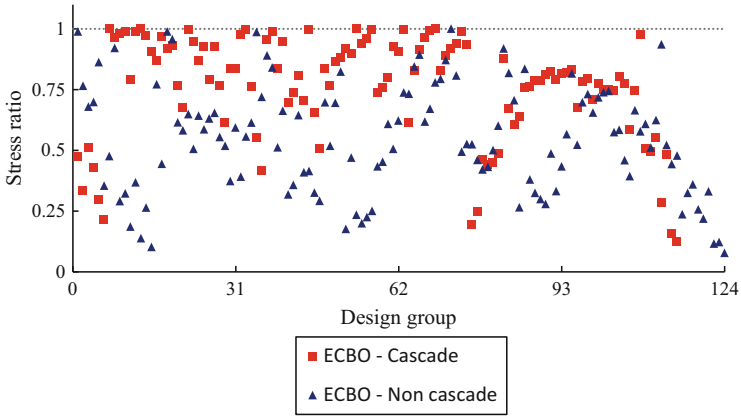

Fig. 19.13 Maximum stress ratio of members in each design group in final design of the 1860-member steel space frame

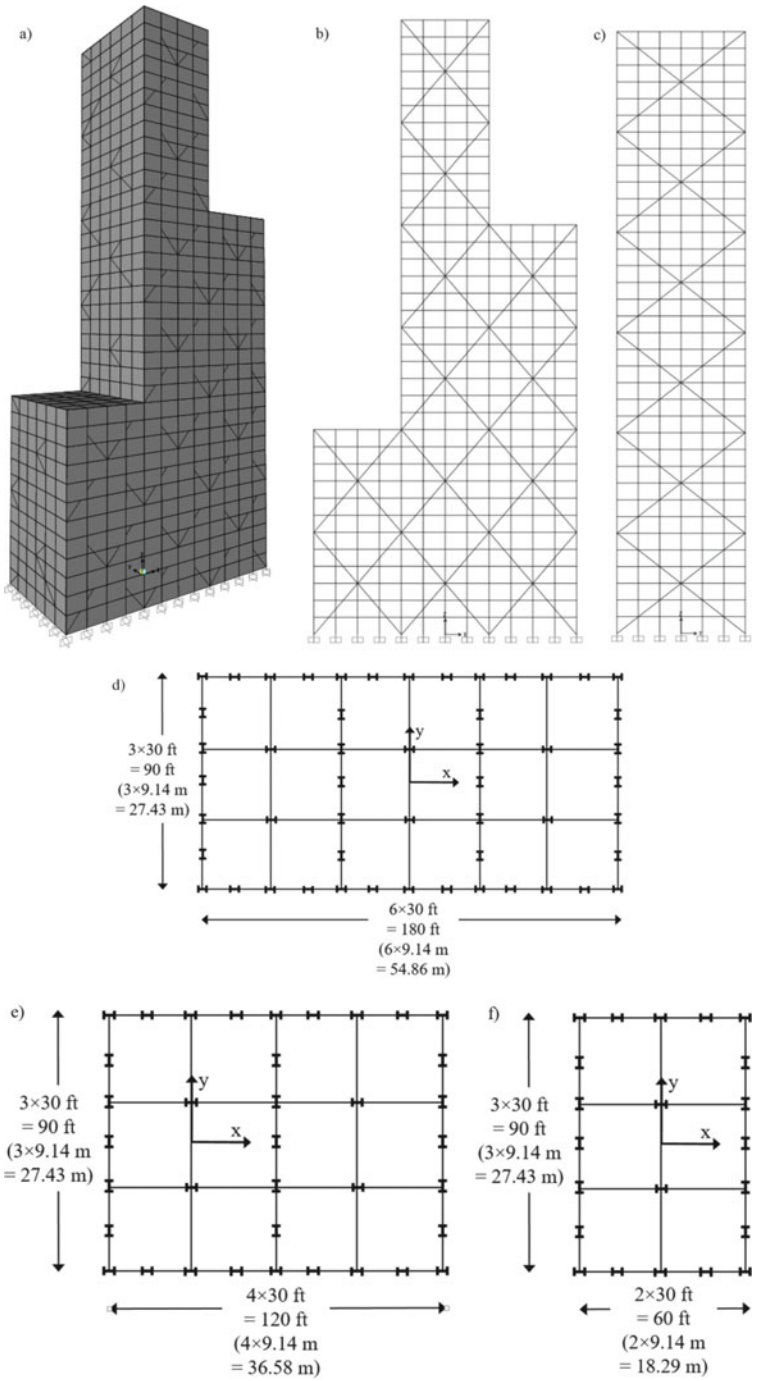

Fig. 19.14 Schematic of a 3328-member braced space steel frame [1]. (**a**) Three-dimensional view, (**b**) front view, (**c**) side view, (**d**) stories 1–12 (Section 1), (**e**) stories 13–24 (Section 2), and (**f**) stories 25–36 (Section 3)

Table 19.7 Wind loading on the 3228-member braced space steel frame

Floor	Windward kN/m (lb/ft)	Leeward kN/m (lb/ft)
1	1.60 (109.41)	2.55 (174.91)
2	1.81 (124.18)	2.55 (174.91)
3	2.03 (139.43)	2.55 (174.91)
4	2.21 (151.37)	2.55 (174.91)
5	2.35 (161.34)	2.55 (174.91)
6	2.48 (169.96)	2.55 (174.91)
7	2.59 (177.62)	2.55 (174.91)
8	2.69 (184.52)	2.55 (174.91)
9	2.78 (190.84)	2.55 (174.91)
10	2.87 (196.67)	2.55 (174.91)
11	2.95 (202.10)	2.55 (174.91)
12	3.02 (207.19)	2.55 (174.91)
13	3.09 (211.98)	2.55 (174.91)
14	3.16 (216.52)	2.55 (174.91)
15	3.22 (220.83)	2.55 (174.91)
16	3.28 (224.94)	2.55 (174.91)
17	3.34 (228.87)	2.55 (174.91)
18	3.39 (232.64)	2.55 (174.91)
19	3.45 (236.26)	2.55 (174.91)
20	3.50 (239.75)	2.55 (174.91)
21	3.55 (243.11)	2.55 (174.91)
22	3.60 (246.36)	2.55 (174.91)
23	3.64 (249.51)	2.55 (174.91)
24	3.69 (252.57)	2.55 (174.91)
25	3.73 (255.53)	2.55 (174.91)
26	3.77 (258.41)	2.55 (174.91)
27	3.81 (261.21)	2.55 (174.91)
28	3.85 (263.94)	2.55 (174.91)
29	3.89 (266.6)	2.55 (174.91)
30	3.93 (269.19)	2.55 (174.91)
31	3.97 (271.73)	2.55 (174.91)
32	4.00 (274.2)	2.55 (174.91)
33	4.04 (276.62)	2.55 (174.91)
34	4.07 (278.99)	2.55 (174.91)
35	4.11 (281.31)	2.55 (174.91)
36	2.07 (141.80)	87.46)

Table 19.8 Gravity loading on the beams of the 3228-member braced steel space frame

	Uniformly distributed load, kN/m (lb/ft)		
Beam type	Dead load	Live load	Snow load
Roof beams	11.12 (761.74)	N/A	3.65 (250.00)
Floor beams	13.26 (908.40)	8.17 (560.00)	N/A

Table 19.9 Number of design variables and their allocation to structural parts for each DVC of the 3228-member braced steel space frame

DVC	Member type	Number of member groups				Total	Remarks
		Section 1	Section 2	Section 3	All sections		
C_0	Columns	$4 \times 6 = 24$	$4 \times 6 = 24$	$3 \times 6 = 18$	66	186	Grouped every two stories
	Beams	$3 \times 12 = 36$	$3 \times 12 = 36$	$2 \times 12 = 24$	96		Grouped every story
	Bracings	$2 \times 4 = 36$	$2 \times 4 = 8$	$2 \times 4 = 8$	24		Grouped every three stories
C_1	Columns	$4 \times 3 = 12$	$4 \times 3 = 12$	$3 \times 3 = 9$	33	81	Grouped every four stories
	Beams	$3 \times 3 = 9$	$3 \times 3 = 9$	$2 \times 3 = 6$	24		Grouped every four stories
	Bracings	$2 \times 4 = 8$	$2 \times 4 = 8$	$2 \times 4 = 8$	24		Grouped every three stories
C_2	Columns	$4 \times 1 = 4$	$4 \times 1 = 4$	$3 \times 1 = 3$	11	25	Grouped every 12 stories
	Beams	$3 \times 1 = 3$	$3 \times 1 = 3$	$2 \times 1 = 2$	8		Grouped every 12 stories
	Bracings	$2 \times 1 = 2$	$2 \times 1 = 2$	$2 \times 1 = 2$	6		Grouped every 12 stories

allowable drift of the story for final design of two mentioned methods for this example. Maximum values of stress ratios for the members of each design group for ECBO and cascade ECBO, for this problem, are also compared in Fig. 19.17.

Predefining of the most critical constraint in optimal design of these problems is almost impossible. In the first example, which is a high-rise regular space frame, drifts in the middle stories are more critical (as expected), but in the second problem, the stress ratios are more critical than other constraints, and in the last example, no specific trends are observed.

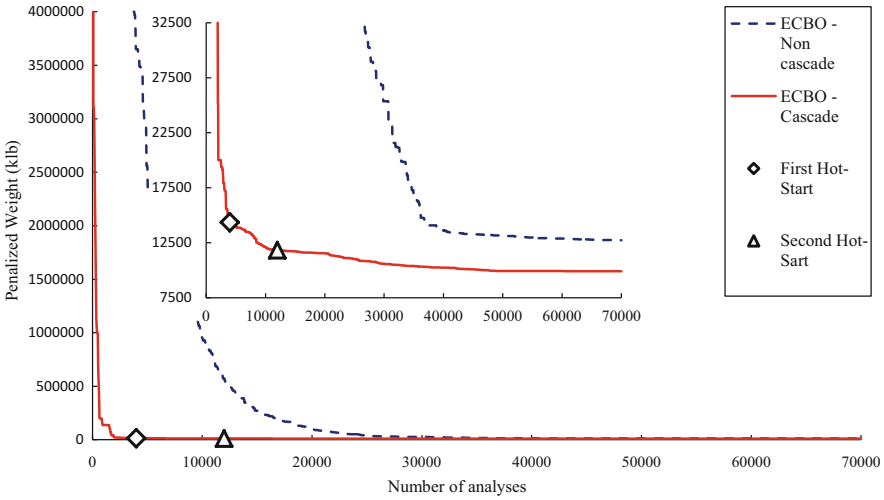

Fig. 19.15 Convergence curves for the 3228-member steel space frame

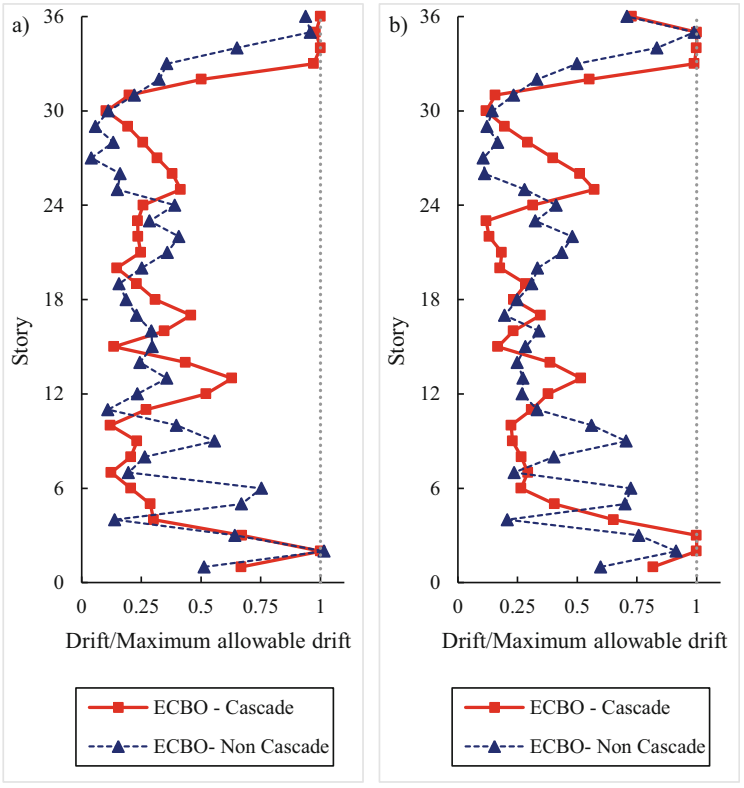

Fig. 19.16 Drift divided by the maximum allowable drift ratio in final design of the 3590-member steel space frame. (**a**) X direction, (**b**) y direction

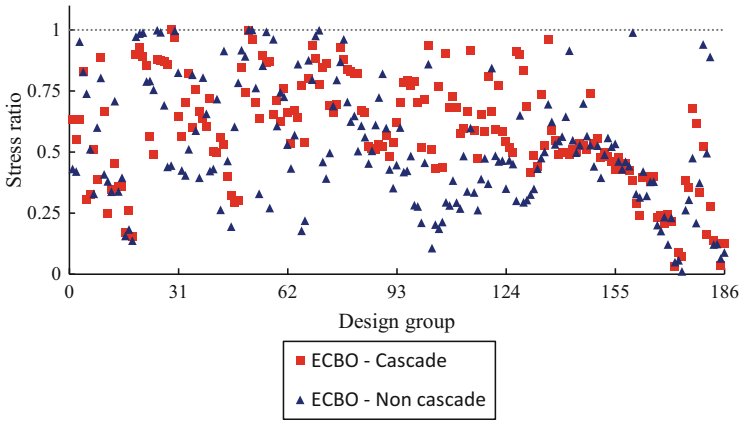

Fig. 19.17 Maximum stress ratio of members in each design group in final design of the 3228-member steel space

19.6 Concluding Remarks

Large-scale steel space frame optimization with design code constraints is a difficult, complex, highly nonlinear, and non-convex problem. In this chapter the performance of multi-DVC cascade and non-cascade ECBO is compared through three large-scale steel space frames. In all examples, in addition to multi-DVC cascade procedure that resulted in better optimized design, the required number of analyses for achieving the best design of non-cascade procedure by the proposed method is decreased. This issue is important due to large computational cost of structural analyses in large-scale steel space frames.

Although ECBO algorithm has shown its efficiency in finding near-optimum solution, however, in problems of this chapter, it did not provide good results. Large number of design variables and nonlinear constraints caused the optimizer to be trapped in local optima. In this condition, optimizer could not find near-optimum solution. Because, finding a variable that its change leads to improvement of the solution, among large number of variables, is a big challenge, and optimizer can hardly cope with this challenge.

References

1. Kaveh A, Bolandgerami A (2016) Optimal design of large scale space steel frames using cascade enhanced colliding body optimization. Struct Multidiscip Optim. 10.1007/s00158-016-1494-2
2. Schulz V, Book HG (1997) Partially reduced sqp methods for large-scale nonlinear optimization problems. Nonlinear Anal Theory Methods Appl 30:4723–4734
3. Dreyer T, Maar B, Schulz V (2000) Multigrid optimization in applications. J Comput Appl Math 120:67–84

4. Wang Q, Arora JS (2007) Optimization of large-scale truss structures using sparse SAND formulations. Int J Numer Methods Eng 69:390–407
5. Yang Z, Tang K, Yao X (2008) Large scale evolutionary optimization using cooperative coevolution. Inf Sci 178:2985–2999
6. Hsieh S-T, Sun T-Y, Liu C-C, Tsai S-J (2008) Solving large scale global optimization using improved particle swarm optimizer. In: Evolutionary computation, 2008. CEC 2008, IEEE World Congress on Computational Intelligence, pp 1777–1784
7. Fister I, Fister Jr I, Zumer JB (2012) Memetic artificial bee colony algorithm for large-scale global optimization. In: IEEE Congress on Evolutionary Computation (CEC), pp 1–8
8. Singh D, Agrawal S (2016) Self organizing migrating algorithm with quadratic interpolation for solving large scale global optimization problems. Appl Soft Comput 38:1040–1048
9. Kaveh A, Talatahari S (2011) Optimization of large-scale truss structures using charged system search. Int J Optim Civ Eng 1(1):15–28
10. Lagaros ND (2013) A general purpose real-world structural design optimization computing platform. Struct Multidiscip Optim 49:1047–1066
11. Talatahari S, Kaveh A (2015) Improved Bat Algorithm for Optimum Design of Large-Scale Truss Structures. Int J Optim Civil Eng 5:241–254
12. Aydoğdu İ, Akın A, Saka MP (2016) Design optimization of real world steel space frames using artificial bee colony algorithm with Levy flight distribution. Adv Eng Softw 92:1–14
13. Papadrakakis M, Lagaros ND, Tsompanakis Y (1998) Structural optimization using evolution strategies and neural networks. Comput Methods Appl Mech Eng 156:309–333
14. Sobieszczanski-Sobieski J, James BB, Dovi AR (1985) Structural optimization by multilevel decomposition. AIAA J 23:1775–1782
15. Sobieszczanski-Sobieski J, James BB, Riley MF (1987) Structural sizing by generalized, multilevel optimization. AIAA J 25:139–145
16. Charmpis DC, Lagaros ND, Papadrakakis M (2005) Multi-database exploration of large design spaces in the framework of cascade evolutionary structural sizing optimization. Comput Methods Appl Mech Eng 194:3315–3330
17. Kaveh A, Ilchi Ghazaan M (2015) Optimal design of dome truss structures with dynamic frequency constraints. Struct Multidiscip Optim. 10.1007/s00158-015-1357-2
18. Kaveh A, Ilchi Ghazaan M (2014) Enhanced colliding bodies optimization for design problems with continuous and discrete variables. Adv Eng Softw 77:66–75
19. Kaveh A, Mahdavi VR (2014) Colliding Bodies Optimization method for optimum design of truss structures with continuous variables. Adv Eng Softw 70:1–12
20. American Institute of Steel Construction (1989) Manual of steel construction: allowable stress design. American Institute of Steel Construction
21. Dumonteil P (1992) Simple equations for effective length factors. Eng J AISC 29(3):111–115
22. Hellesland J (1996) Improved frame stability analysis with effective lengths. J Struct Eng 122 (11):1275–1283
23. Specification A (2005) Specification for structural steel buildings. ANSI/AISC
24. Patnik SN, Coroneos RM, Hopkins DA (1997) A cascade optimization strategy for solution of difficult design problems. Int J Numer Methods Eng 40:2257–2266
25. The MathWorks (2013) MATLAB, Natick, Massachusetts, USA
26. Mazzoni S, McKenna F, Scott M (2006) OpenSees command language manual
27. Saka MP, Hasancebi O (2009) Adaptive harmony search algorithm for design code optimization of steel structures. Springer, Berlin
28. Sarma KC, Adeli H (2002) Life-cycle cost optimization of steel structures. Int J Numer Methods Eng 55:1451–1462